

## Author Manuscript

**Title:** Mesoporous high surface area Cu-Sn mixed oxide nano-rods: remarkable for CO oxidation

**Authors:** Honggen Peng; Yang Liu, B.S.; Yarong Li; Xianhua Zhang; Xianglan Tang; Xianglan Xu; Xiuzhong Fang; Wenming Liu; Ning Zhang; Xiang Wang

This is the author manuscript accepted for publication and has undergone full peer review but has not been through the copyediting, typesetting, pagination and proofreading process, which may lead to differences between this version and the Version of Record.

**To be cited as:** 10.1002/cctc.201600221

**Link to VoR:** <http://dx.doi.org/10.1002/cctc.201600221>

# Mesoporous high surface area Cu-Sn mixed oxide nano-rods: remarkable for CO oxidation

Honggen Peng,<sup>a,b</sup> Yang Liu,<sup>a</sup> Yarong Li,<sup>a</sup> Xianhua Zhang,<sup>a</sup> Xianglan Tang<sup>a</sup>, Xianglan Xu,<sup>a</sup> Xiuzhong Fang,<sup>a</sup> Wenming Liu,<sup>a</sup> Ning Zhang,<sup>a</sup> Xiang Wang<sup>\*a</sup>

**Abstract:** Mesoporous high surface area Cu-Sn mixed oxide nanorod was facially fabricated for the first time *via* nanocasting method by using mesoporous KIT-6 silica as the hard template. Cu-Sn nanorod shows significantly higher activity than 1% Pd/SnO<sub>2</sub> for CO oxidation, and possesses long term durability and potent water-resistance, which has the potential to replace noble metal catalysts for emission control processes.

The morphology of a catalyst is critical for its catalytic performance, therefore, morphology control has become a popular strategy to improve the activity, selectivity, and stability of a catalyst over recent years<sup>1-9</sup>. Metal oxide catalysts with elongated rod-shape structure have generally many advantages, such as higher surface to volume ratio, preferentially exposed active facets and improved mechanical stability, which are key factors to determine the application potential of the catalysts<sup>6, 10-12</sup>. Shen and co-workers<sup>13</sup> reported that Co<sub>3</sub>O<sub>4</sub> nano-rods not only catalyze CO oxidation at temperature as low as -77 °C but also remain very stable in a moisture stream. MnO<sub>2</sub> nano-rods prepared by hydrothermal method also showed much better catalytic performance for toluene combustion than the counterpart polycrystalline powder prepared by precipitation method<sup>14</sup>. Rod-like CeO<sub>2</sub> was also studied as support for Au and NiO to prepare catalysts for preferential CO oxidation in H<sub>2</sub>-rich gas<sup>4</sup> and NO selective reduction with NH<sub>3</sub><sup>15</sup>, respectively, both showing improved reaction performance. In addition, it was reported that Mn-Ce mixed oxide nano-rods with high content of Mn also display very high activity and stability for toluene combustion.<sup>16</sup>

Our group has previously reported that pure SnO<sub>2</sub> nano-rod shows much improved activity for CO oxidation in comparison with other morphologies.<sup>17</sup> Most importantly, its catalytic behavior is similar to that of supported noble metal catalysts. Although specific surface area of this SnO<sub>2</sub> nano-rod catalyst is as low as 1 m<sup>2</sup> g<sup>-1</sup> and it contains no any active oxygen species, it has preferentially exposed [110] facets, which have been testified formerly by other researchers to be the active facets.<sup>17</sup> Whereas, the activity of this SnO<sub>2</sub> nano-rod catalyst is still lower than the comparison sample, 1% Pd/SnO<sub>2</sub>. If its activity can be further improved, SnO<sub>2</sub> nano-rod itself could be a good candidate to replace the noble metal catalysts. Very recently, mesoporous SnO<sub>2</sub> and Cu-Sn mixed oxide nano-sheets have been successfully prepared by our group, which show superior activity and stability for CO oxidation at low temperature due to the presence of a

large amount of mobile oxygen species and also their high surface areas.<sup>18</sup> The creation of mesopores in SnO<sub>2</sub> nano-rod could also increase its surface area, produce mobile oxygen species and enhance the contacting of the reactants with the active sites, thus eventually improving its activity and achieving catalysts with competitive performance to that of noble metals. Nanocasting technology is a versatile method to create nonsiliceous nanostructured porous materials.<sup>19</sup> In a casting process, usually, a replica structure can be obtained, which is the negative replica. Until now, to the best of our knowledge, there was little research on using mesoporous silica as hard template to prepare mesoporous mixed oxide nano-rod *via* nanocasting strategy.

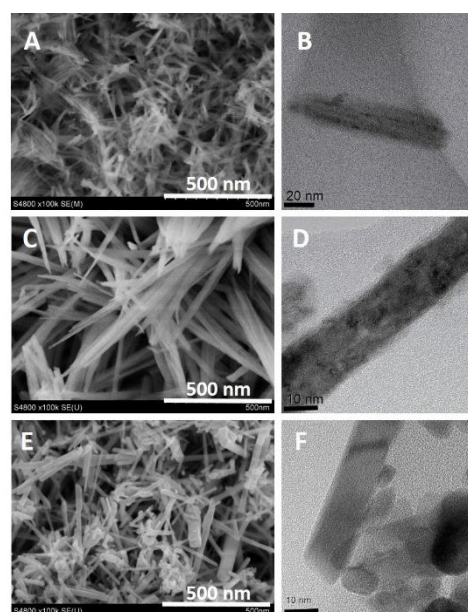


**Figure 1** SEM (left) and TEM (right) images of Cu-Sn nano-rods (molar ratio of Cu : Sn=1 : 1) calcined at 300 (A, B), 400 (C, D) and 550 °C (E, F).

In this communication, a mesoporous silica, KIT-6, with ordered mesopores (**Figure S1-3**) was synthesized and used as the hard template to prepare Cu-Sn metal oxide nano-rods with a Cu/Sn molar ratio of 1/1 *via* nano-casting method<sup>19-21</sup> for the first time, and used for CO oxidation after calcination at different temperatures. The detailed preparation procedures and the reaction condition are described in the ESI.

SEM and TEM images in **Figure 1** demonstrate that the Cu-Sn mixed oxide calcined at different temperatures has rod-like morphology. With the increasing of the temperature from 300 to 400 °C, the nano-rod becomes elongated and neater. However, further increasing the calcination temperature to 550 °C obviously induces the formation of some polycrystalline metal oxide powder, indicating part of the rod structure was damaged. As shown in the TEM images in **Figure 1(D)**, on the Cu-Sn nano-rod calcined at 400 °C, some mesopores are present, which was further confirmed by the N<sub>2</sub>

[a] Institute of Applied Chemistry, College of Chemistry, Nanchang University, Nanchang, Jiangxi 330031, China. E-mail: xwang23@ncu.edu.cn (X. Wang)

[b] School of Chemistry and Chemical Engineering, Shanghai Jiao Tong University, 800 Dongchuan Road, Shanghai 200240, China.

Supporting information for this article is given via a link at the end of the document.

adsorption-desorption results in **Figure S4**. As listed in **Table S1**, the three samples calcined at different temperatures have similar pore sizes, which are around 4 nm. Due to the formation of mesoporous structure, the surface areas of all the three samples are above 110 m<sup>2</sup>/g, which are much larger than the un-modified SnO<sub>2</sub> nano-rod prepared formerly by our group with molten salt method.<sup>17</sup> Apparently, the mesoporous structure and high surface areas are favorable for the activity of the catalysts.

Usually, using mesoporous silica as hard template and metal oxide as precursor, after removing the template by NaOH or HF, a replica of metal oxide was obtained via nanocasting method. However, in this communication, a novel mesoporous mixed oxide nano-rod was formed by using nanocasting method. From the TEM images of Cu-Sn mixed oxide nano-rods, the size of the cross section of the rods is about 10 nm, which is very similar to the pore size of KIT-6 (average pore size is 7.8 nm, **Figure S2**), so the rod shape structure might be formed by metal precursor grown along the main cylindrical pores of KIT-6 (**Figure S1 C**), though KIT-6 is a bi-continuous cubic Ia3d meso-silica.

To elucidate the phase compositions of the Cu-Sn nano-rods, XRD patterns of the samples were compared with the individual SnO<sub>2</sub> and CuO in **Figure S5**. All the Cu-Sn nano-rods show obviously the diffraction features of tetragonal rutile SnO<sub>2</sub> phase, indicating that the major part of the Cu cations could have incorporated into its lattice to form solid solution structure.<sup>18, 22</sup> To confirm this, the 2 $\theta$  and *d* values of the two strongest peaks of rutile SnO<sub>2</sub> phase, peak (110) and (101), in the Cu-Sn nano-rod samples are identified carefully and compared in **Table S2**. As reported formerly<sup>23, 24</sup>, Cu<sup>2+</sup> with a coordination number (CN) of 6 has a radius of 0.074 nm, while that of Sn<sup>4+</sup> with the same CN is 0.069 nm. In comparison with individual SnO<sub>2</sub>, both the two diffraction peaks shift to lower angles but the *d* values increase, testifying the expansion of the distance between the crystal facets by the incorporation of bigger Cu<sup>2+</sup> cations into the crystal lattice of SnO<sub>2</sub>. Indeed, this proves further that a considerable amount of the Cu cations have been introduced into the SnO<sub>2</sub> lattice to form solid solution structure. However, the valence state difference between the two cations is relatively big. As a result, Cu<sup>2+</sup> cations can only be dissolved into the SnO<sub>2</sub> lattice with a certain capacity.<sup>25</sup> With a Cu/Sn molar ratio of 1/1, the amount of Cu cations obviously exceeds the capacity. Therefore, Cu(OH)<sub>2</sub> phase is observed for CuSn-Rod-300 and CuO is observed for CuSn-Rod-400 and CuSn-Rod-550 as the minor phases. It is also noted here that with the increasing of the calcination temperature, the mean crystallite size of the SnO<sub>2</sub> phase becomes larger, indicating the better crystallization of the formed Cu-Sn solid solution.

displayed in **Figure 2(B, C and D)** in sequence. It is revealed that the three elements distribute very uniformly in the sample, confirming that homogeneous solid solution structure has been formed in the Cu-Sn mixed oxide nano-rods.

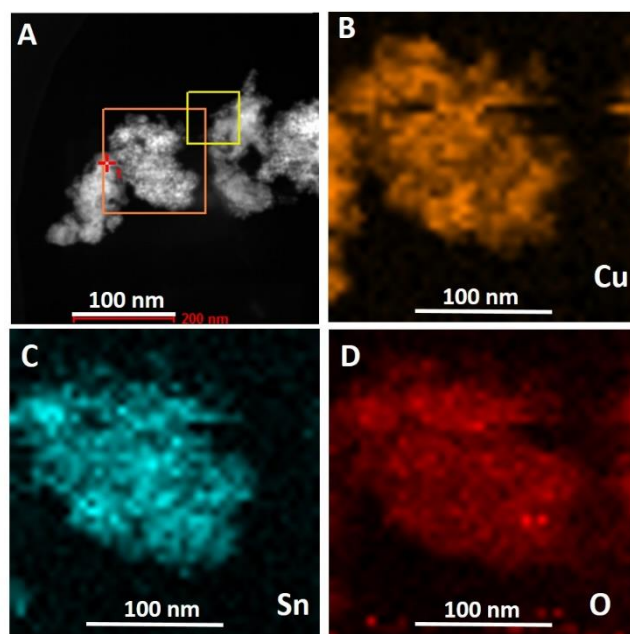


**Figure 2** HAADF STEM image (A) and elemental mapping of mesoporous Cu-Sn nano-rod (molar ratio of Cu : Sn=1 : 1) calcined at 400 °C in air (B, C, D).

The redox properties of the samples were studied by H<sub>2</sub>-TPR, with the profiles shown in **Figure S6**, and the H<sub>2</sub> uptake amount quantified in **Table 1**. For all the Cu-Sn nano-rod samples calcined at different temperatures, three groups of reduction peaks can be distinctly observed below 240 °C, around 380 °C and above 540 °C, respectively. The peak below 240 °C is assigned to the reduction of CuO species in the samples into metallic Cu<sup>18</sup>. In contrast, the peak above 530 °C is assigned to the reduction of SnO<sub>2</sub> to metallic Sn<sup>17</sup>. Whereas, the small peak around 380 °C is believed to be the reduction of deficient oxygen species induced by the formation of Cu-Sn solid solution structure in the samples<sup>18</sup>. With the variation of the calcination temperature, the reduction behaviour of the samples is obviously changed. For low temperature CO oxidation, the oxygen species reduced at low temperature is believed to be critical for the activity of a catalyst if it follows Mars-van Krevlen mechanism<sup>26</sup>.

**Table 1** The reaction performance and quantified H<sub>2</sub>-TPR and XPS results of mesoporous CuSn nano-rod (molar ratio of Cu : Sn=1 : 1) catalysts

| Samples      | H <sub>2</sub> consumption (mmol g <sup>-1</sup> ) |         |          | Total | O <sub>ads</sub> /O <sub>lat</sub><br>(XPS) | Reaction   |  |                               |
|--------------|--|---------|----------|-------|---|--|--|-------------------------------|
|              | <240 °C  | ~380 °C | > 530 °C |       |   | Rate<br>(10 <sup>-4</sup> mmol g <sup>-1</sup> s <sup>-1</sup> ) | Rate<br>(10 <sup>-6</sup> mmol m <sup>-2</sup> s <sup>-1</sup> ) | Ea<br>(kJ mol <sup>-1</sup> ) |
| CuSn-rod-300 | 2.5  | 0.7     | 5.7      | 8.9   | 0.6   | 0.3  | 0.114  | 66.5                          |
| CuSn-rod-400 | 3.8  | 1.1     | 3.8      | 8.7   | 2.7   | 9.2  | 5.9  | 47.3                          |
| CuSn-rod-550 | 3.6  | 0.8     | 3.6      | 8.0   | 1.5   | 4.9  | 4.3  | 50.3                          |

To further clarify the formation of solid solution structure between Cu and Sn oxides, CuSn-Rod-400, the typical catalyst in this study was thus measured by HAADF STEM mapping, with the image shown in **Figure 2**. The mapping zone is labelled in the SEM image in **Figure 2(A)**, while the elemental distribution of Cu, Sn and O elements is

While the total H<sub>2</sub> consumption amount of the samples decreases from 8.9 to 8.0 mmol/g, the amount of the first two low temperature peaks is 3.2, 4.9 and 4.4 mmol/g for CuSn-Rod-300, CuSn-Rod-400 and CuSn-Rod-550, respectively. Apparently, CuSn-Rod-400, the sample calcined at 400 °C obviously consumes the largest amount

of hydrogen at around 240 and 380 °C, indicating this sample contains the largest amount of active oxygen species, which are believed to be favourable for CO oxidation. In comparison, CuSn-Rod-300, the sample calcined at 300 °C, possesses the smallest amount of these active oxygen species, possibly due to the still presence of a large quantity of OH groups.

XPS technique was adopted to identify the surface composition of the catalysts, with the spectra displayed in **Figure S7**. The binding energies observed in **Figure S7(A)** and **(B)** for  $\text{Cu}_{2p}$  and  $\text{Sn}_{3d}$  are typical for  $\text{Cu}^{2+}$  and  $\text{Sn}^{4+}$ <sup>18</sup>, which is in line with the  $\text{H}_2$ -TPR results. The asymmetric  $\text{O}_{1s}$  peaks of the samples shown in **Figure S7(C)** indicate the presence of surface oxygen species with different chemical environments. Therefore, the  $\text{O}_{1s}$  peaks of the samples are deconvoluted and shown in **Figure S7(D-F)**. While the peak around 530 eV is assigned to surface lattice oxygen ( $\text{O}_{\text{lat}}$ )<sup>27</sup>, the peak around 532 eV is attributed to loosely bonded surface oxygen species ( $\text{O}_{\text{ads}}$ )<sup>27</sup>, which is believed to be important for the oxidation activity of the catalysts. Therefore, the  $\text{O}_{\text{ads}}/\text{O}_{\text{lat}}$  ratios of the samples are quantified and listed in **Table 1**. Apparently, CuSn-rod-400, the sample calcined at 400 °C, possesses the highest value, testifying further that this sample has the largest amount of active oxygen vacancies. Indeed, the XPS results are in agreement with what was detected by the  $\text{H}_2$ -TPR experiments.

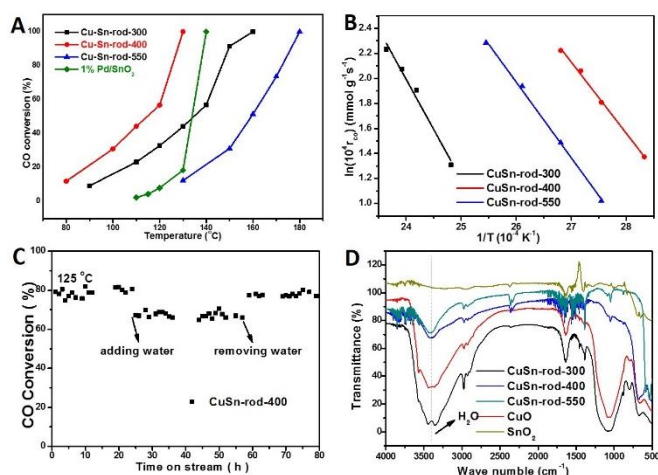


**Figure 3** (A) CO conversion versus reaction temperatures, (B) Arrhenius plots, (C) Stability test in the absence or presence of water vapor and (D) FTIR spectra of the Cu-Sn nano-rod samples (molar ratio of Cu : Sn = 1 : 1) after water adsorption.

The activity of the catalysts was evaluated by CO oxidation. As shown in **Figure 3(A)**, CuSn-Rod-400, the sample calcined at 400 °C, displays the highest overall activity, on which the complete CO conversion occurred at 130 °C. In comparison with the pure  $\text{SnO}_2$  nano-rod prepared by us, this temperature is 130 °C lower<sup>17</sup>. Furthermore, its overall activity is even higher than that of 1%  $\text{Pd}/\text{SnO}_2$ , the comparison catalyst, which achieves complete CO oxidation at 140 °C (**Figure 3A**). It is obvious that with the combination of Cu and Sn oxides, Cu-Sn nano-rods with higher activity than supported Pd can be obtained.

CuSn-Rod-300, the sample calcined at 300 °C, though has the highest surface area among the three samples, exhibits the lowest overall activity, indicating surface area is not the determining factor for the activity of the catalysts. To elucidate the inherent reasons accounting for the activity, the differentiate rates on the samples were collected and plotted as Arrhenius plots in **Figure 3(B)**. Although CuSn-Rod-400 and CuSn-Rod-550 have evidently lower surface areas than CuSn-Rod-300, they have significantly higher

reaction rates under differential condition. For easy comparison, the differentiate rate at 100 °C for each sample is listed in **Table 1** together with the overall activation energy. It is revealed that the two samples calcined at higher temperatures have not only higher rates but also lower activation energies. This strongly indicates that more reactive sites have been formed in these two catalysts. As described above, XRD phase analysis indicates that on CuSn-Rod-300,  $\text{Cu}(\text{OH})_2$  phase is detected instead of  $\text{CuO}$  phase due to the low calcination temperature. It is reasonable to deduce that in this sample, a large amount of OH groups are still present, which could influence the effective formation of solid solution structure, as testified by the less shift of  $2\theta$  and  $d$  values. As a result, smaller amount of active oxygen species is formed, as evidenced by  $\text{H}_2$ -TPR and XPS results. In contrast, with the increasing of the calcination temperature to 400 °C, a larger amount of active oxygen species has been produced, but which will be partly destroyed by further increasing the temperature to 550 °C due to better crystallization. As a consequence, CuSn-Rod-400, the sample calcined at 400 °C displays the highest activity among all the samples.

In real exhausts, 5-10% water vapour is generally present, therefore, CuSn-Rod-400, the optimal catalyst in this study, was subjected to a long-term stability test in the absence or presence of 5% water vapour. As shown in **Figure 3(C)**, after the addition of 5% water vapour, the CO conversion has about 10% decrease, which can be completely restored after removing the water vapour. This indicates that the CuSn-Rod-400 is not only stable but also water resistant. FTIR technique was thus used to investigate the water adsorption behaviours of the samples, with the spectra shown in **Figure 3(D)**. After saturation in water vapour and followed by purging by He flow to remove any physically adsorbed water, while pure  $\text{CuO}$  displays an evident water adsorption peak at  $\sim 3350 \text{ cm}^{-1}$ , individual  $\text{SnO}_2$  shows no any adsorption of water molecules<sup>27</sup>. It is particularly noted here that due to the initial presence of a large amount of OH groups in its structure, CuSn-Rod-300 displays a big peak at  $3350 \text{ cm}^{-1}$ . However, although CuSn-Rod-400 and CuSn-Rod-550 also display a water adsorption peak at the same wavenumber, whose integrated areas are much smaller in comparison with that of pure  $\text{CuO}$ , indicating the combination of Cu and Sn oxides can achieve catalysts with significantly improved water tolerance.

In summary, mesoporous high surface area Cu-Sn mixed oxide nano-rods were successfully fabricated by using mesoporous silica (KIT-6) as the hard template for the first time. Cu cations were found to be incorporated into the crystal lattice of rutile  $\text{SnO}_2$  to form solid solution structure, which induced the formation of more active oxygen species. CuSn-Rod-400, the nano-rod sample calcined at 400 °C, displays the highest activity for CO oxidation, which is even higher than a comparison Pd catalyst (1%  $\text{Pd}/\text{SnO}_2$ ) under the same condition. Last but not the least, Cu-Sn nano-rod catalysts show also superior stability and water-resistance, which makes them potential catalysts to replace precious metal catalysts for real exhaust clean.

## Experimental Section

**Synthesis of mesoporous silica KIT-6 hard template.** The mesoporous silica template with cubic Ia3d bicontinuous structure (KIT-6) was prepared according to the literatures [1, 2]. Typically, 9 g P123 ( $\text{EO}_{20}\text{PO}_{70}\text{EO}_{20}$ , Mw=5800, Aldrich) was dissolved in 326 g distilled ionized (DDI) water and 17.7 g concentrated HCl (35%~37%). Then, 9 g butanol (>99%) was added under constant stirring at 35 °C. After stirring about 1 h, 19.4 g tetraethyl orthosilicate (TEOS, 98%) was added to the above solution. The mixture was continuously stirred for another 24 h at

35 °C, and subsequently transferred to a 500 ml Teflon-lined stainless-steel autoclave and heated at 100 °C for 24 h under static conditions. The white precipitates recovered by filtration were thoroughly washed with distilled deionized water followed by drying at 90 °C overnight. The P123 was removed by calcining the as-made materials at 550 °C for 6 h in air.

#### Synthesis of mesoporous Cu-Sn nano-rod via nanocasting method.

Typically, 3.02 g  $\text{Cu}(\text{NO}_3)_2 \cdot 3\text{H}_2\text{O}$  (12.5 mmol) and 4.38 g  $\text{SnCl}_4 \cdot 5\text{H}_2\text{O}$  (12.5 mmol) were dissolved into 10 ml absolute ethanol, then 2.5 g KIT-6 (calcined at 200 °C in vacuum) was added and the mixture was stirred for 1 h at room temperature. Afterwards, the temperature was increased to 60 °C in water bath with continuous stirring until the solvent was evaporated. The powder was dried at 60 °C for 12 h and then calcined at 200 °C for 4 h with a heating rate of 1 °C  $\text{min}^{-1}$ . The above procedures were repeated except that the solution mixture consists of 1 g  $\text{Cu}(\text{NO}_3)_2 \cdot 3\text{H}_2\text{O}$ , 1.5 g  $\text{SnCl}_4 \cdot 5\text{H}_2\text{O}$  and 5 ml absolute ethanol. The obtained sample was then calcined at 300 °C, 400 °C and 550 °C for 4 h, respectively. After this, the silica template (KIT-6) was removed with an aqueous NaOH (2 M) solution at 65 °C for 6 h. This etching step was repeated to ensure that the silica template was completely removed. The achieved samples were then dried thoroughly at 90 °C overnight. The final samples are named as CuSn-rod-300, CuSn-rod-400 and CuSn-rod-550, respectively. The element compositions of the samples are identified by ICP technique, with the results listed in Table S1. It is noted that for the samples calcined at 400 and 550 °C, the Cu/Sn molar ratios are around 1/1, as designed. However, for the sample calcined at 300 °C, part of the Cu species was lost during the etching process, due to the low calcination temperature, which results in a Cu/Sn molar ratio of 0.81.

**Catalyst characterization.** The Powder X-ray diffraction (XRD) patterns were recorded on a Bruker AXS D8Focus diffractometer operating at 40 kV and 30 mA, with a Cu target  $\text{K}\alpha$ -ray irradiation ( $\lambda = 1.5405 \text{ \AA}$ ). Scans were taken with a  $2\theta$  range from 10 to 90° for wide angle scan with a step of 5°  $\text{min}^{-1}$ , and 0.5 to 6° for small angle scan with a step of 1°  $\text{min}^{-1}$ . To keep the data comparable, all of the samples were tested continuously under the same condition. The mean crystallite sizes of the samples were calculated with Scherrer equation based on the three strongest peaks of  $\text{SnO}_2$  with hkl of (110), (101) and (211). The calculated experimental error for  $2\theta$  measurement of the peaks is  $\pm 0.01^\circ$ , which ensures the reliable identification of peak shift observed by solid solution formation. The copper and tin contents were determined by inductively coupled plasma atomic emission spectroscopy (ICP-AES) on an IRIS Intrepid II XSP instrument (Thermo Electron Corporation). The scanning electron microscope (SEM) images were taken on a Hitachi S-4800 field emission scanning electron microscope. The Transmission Electron Microscope (TEM) images were taken on a Tecnai™ F30 transmission electron microscope. The high angle annular dark field scanning transition electron microscopy (HAADF-STEM) images, elemental phase mapping and surface scans by energy-dispersive spectroscopy (EDS) were also obtained using a Tecnai™ F30 transmission electron microscope equipped with an Oxford EDX detector operated at 300 keV. Nitrogen adsorption-desorption of the samples were carried out at 77 K on ASAP2020 instrument. The specific surface areas of the samples were calculated using Brunauer-Emmett-Teller (BET) method in the relative pressure ( $P/P_0$ ) range of 0.05-0.25. The pore size distributions of the samples were calculated with Barrett-Joyner-Halenda (BJH) method. The average pore sizes of the samples were obtained from the peak positions of the distribution curves. The total pore volume of each catalyst was accumulated at a relative pressure of  $P/P_0 = 0.99$ . Hydrogen temperature programmed reduction ( $\text{H}_2$ -TPR) experiments were carried out on FINESORB 3010C instrument in a 30 ml  $\text{min}^{-1}$  10%  $\text{H}_2/\text{Ar}$  gas mixture flow. Generally, 50 mg catalysts were used for the tests. Prior to the experiments, the catalysts were re-calcined in a high purity air flow at 300 °C for 30 min to remove any surface impurities. The temperature was then increased from room temperature to 850 °C with a rate of 10 °C  $\text{min}^{-1}$ . A thermal conductivity detector (TCD) was employed to monitor the  $\text{H}_2$  consumption. For  $\text{H}_2$  consumption quantification, CuO (99.99%) was used as the calibration standard. X-ray Photoelectron Spectroscopy (XPS) test was carried out on a PerkinElmer PHI1600

system using a single Mg-K-X-ray source operating at 300 W and 15 kV. The spectra were obtained at ambient temperature with an ultrahigh vacuum. The binding energies were calibrated using the C 1s peak of graphite at 284.5 eV as a reference. FTIR was recorded in a range of 500-4000  $\text{cm}^{-1}$  on a Nicolet Nexus 670 FT-IR spectrometer in absorbance mode at a spectral resolution of 2  $\text{cm}^{-1}$  at room temperature. To measure the water adsorption, the fresh samples were saturated in water vapour prior to the experiments, and subsequently purged by an ultra-high purity He flow for 30 min to remove any physically adsorbed water.

**Activity evaluation.** The catalytic performance of the catalysts was evaluated by CO oxidation with a U-shaped quartz tube (ID=6 mm) reactor with a down flow over 100 mg catalyst. Typically, 0.3-0.4 mm catalyst particles were used for activity test. A K-type thermocouple was placed on top of the catalyst bed with the thermocouple head point touching the catalyst to monitor the reaction temperature. To measure the light-off behaviours of the catalysts, all data were collected with increasing the temperature. The volume composition of the feed gas is 1% CO, 21%  $\text{O}_2$  and balanced by high purity  $\text{N}_2$ , with a flow rate of 40 ml  $\text{min}^{-1}$ , which corresponds to a space velocity of 24,000  $\text{ml h}^{-1} \text{ g}_{\text{cat}}^{-1}$ . The reactants and products were analysed on-line on a GC9310 gas chromatograph equipped with a TDX-01 column and a TCD detector. To get steady state kinetic data, the reaction at each temperature was stabilized at least 30 min before analysis. The flow rate of the  $\text{H}_2$  carrier gas is 30 ml  $\text{min}^{-1}$ .

## Acknowledgements

This work was supported by National Natural Science Foundation of China (21263015, 21567016 and 21503106), the Education Department of Jiangxi Province (KJLD14005) and the Natural Science Foundation of Jiangxi Province (20142BAB213013, 20151BAB203024 and 20151BBE50006), which is greatly acknowledged by the authors.

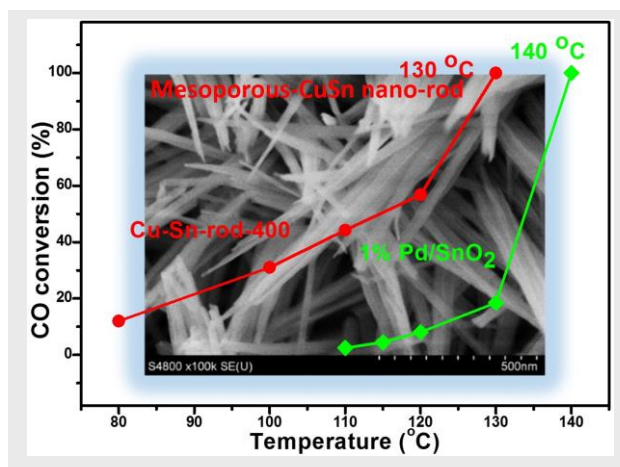
**Keywords:** Cu-Sn mixed oxides • Nano-rods • Mesoporous • CO oxidation • Superior activity

1. W. Huang and Y. Gao, *Catal. Sci. Technol.*, 2014, **4**, 3772-3784.
2. T. Nguyen, C. Dinh and T. Do, *Chem. Commun.*, 2015, **51**, 624-635.
3. Z. Dou, C. Cao, Y. Chen and W. Song, *Chem. Commun.*, 2014, **50**, 14889-14891.
4. G. Yi, Z. Xu, G. Guo, K. Tanaka and Y. Yuan, *Chem. Phys. Lett.*, 2009, **479**, 128-132.
5. Y. Li and W. Shen, *Chem. Soc. Rev.*, 2014, **43**, 1543-1574.
6. P. Hu, M. E. Schuster, Z. Huang, F. Xu, S. Jin, Y. Chen, W. Hua, D. S. Su and X. Tang, *Chem. Eur. J.*, 2015, **21**, 9619-9623.
7. A. Pendashteh, S. E. Moosavifar, M. S. Rahmanifar, Y. Wang, M. F. El-Kady, R. B. Kaner and M. F. Mousavi, *Chem. Mater.*, 2015, **27**, 3919-3926.
8. F. Wang, H. Dai, J. Deng, G. Bai, K. Ji and Y. Liu, *Environ. Sci. Technol.*, 2012, **46**, 4034-4041.
9. H. Kim and J. Cho, *J. Mater. Chem.*, 2008, **18**, 771-775.
10. G. Chen, Q. Xu, Y. Yang, C. Li, T. Huang, G. Sun, S. Zhang, D. Ma and X. Li, *ACS Appl. Mater. Inter.*, 2015, **7**, 23538-23544.
11. S. Zhang, C. Chang, Z. Huang, Y. Ma, W. Gao, J. Li and Y. Qu, *ACS Catal.*, 2015, **5**, 6481-6488.
12. S. Zhuo, J. Zhang, Y. Shi, Y. Huang and B. Zhang, *Angew. Chemie. Inter. Ed.*, 2015, **54**, 5693-5696.
13. X. Xie, Y. Li, Z. Liu, M. Haruta and W. Shen, *Nature*, 2009, **458**, 746-749.

14. F. Shi, F. Wang, H. Dai, J. Dai, J. Deng, Y. Liu, G. Bai, K. Ji and C. T. Au, *Appl. Catal. A- Gen.*, 2012, **433-434**, 206-213.
15. P. Maitarad, J. Han, D. Zhang, L. Shi, S. Namuangruk and T. Rungrotmongkol, *J Phys. Chem. C*, 2014, **118**, 9612-9620.
16. Y. Liao, M. Fu, L. Chen, J. Wu, B. Huang and D. Ye, *Catal. Today*, 2013, **216**, 220-228.
17. X. Wang, L. Xiao, H. Peng, W. Liu and X. Xu, *J. Mater. Chem. A*, 2014, **2**, 5616-5619.
18. Y. Li, H. Peng, X. Xu, Y. Peng and X. Wang, *Rsc Adv.*, 2015, **5**, 25755-25764.
19. A. H. Lu and F. Schüth, *Adv. Mater.*, 2006, **18**, 1793-1805.
20. D. Gu and F. Schuth, *Chem. Soc. Rev.*, 2014, **43**, 313-344.
21. B. Tian, X. Liu, H. Yang, S. Xie, C. Yu, B. Tu and D. Zhao, *Adv. Mater.*, 2003, **15**, 1370-1374.
22. M. J. Fuller and M. E. Warwick, *J. Chem. Soc., Chem. Commun.*, 1973, 210a.
23. X. Xu, R. Zhang, X. Zeng, X. Han, Y. Li, Y. Liu and X. Wang, *ChemCatchem*, 2013, **5**, 2025-2036.
24. M. Luo, J. Ma, J. Lu, Y. Song and Y. Wang, *J. Catal.*, 2007, **246**, 52-59.
25. X. Xu, F. Liu, X. Han, Y. Wu, W. Liu, R. Zhang, N. Zhang and X. Wang, *Catal. Sci. Technol.*, 2016.
26. Y. Liu, H. Dai, Y. Du, J. Deng, L. Zhang, Z. Zhao and C. T. Au, *J. Catal.*, 2012, **287**, 149-160.
27. X. Xu, X. Sun, H. Han, H. Peng, W. Liu, X. Peng, X. Wang and X. Yang, *Appl. Surf. Sci.*, 2015, **355**, 1254-1260.

## COMMUNICATION

**Cu-Sn nano-rod, rival to Pd catalysts:** Mesoporous high surface area Cu-Sn nano-rod was successfully fabricated for the first time via nanocasting method by using KIT-6 silica as the hard template, which shows significantly higher activity than 1% Pd/SnO<sub>2</sub> for CO oxidation, and has the potential to replace noble metal catalysts for



Honggen Peng, Xianhua Zhang, Yarong Li, Xianglan Tang, Xianglan Xu, Xiuzhong Fang, Wenming Liu, Ning Zhang, Xiang Wang\*

Page No. – Page No.

Mesoporous high surface area Cu-Sn mixed oxide nano-rods: remarkable for CO oxidation

Author Manuscript